

Thermodynamic Modeling of the Advanced Geothermal System using Inclined Well Applications

Wanju Yuan, Zhuoheng Chen, Stephen E. Grasby, and Gang Zhao

Geological Survey of Canada, 3303 33 Street NW, Calgary, Alberta Canada T2L 2A7

wanju.yuan@NRCan-RNCan.gc.ca

Keywords: Advanced geothermal system, Closed-loop technology, Inclined wellbores, Thermodynamic modeling, Sensitive analysis

ABSTRACT

The advanced geothermal system (AGS), also called the closed-loop geothermal technology, has advantages of being independent of available reservoir fluids and good permeability, stable energy output, and has already widely been used in shallow geothermal systems for space heating purposes and pilot tested in the deep underground for the electricity power generation purpose. Commercial success requires extreme long horizontal wellbore completion and high reservoir temperature, limiting its application to power generation in sedimentary basins. Reaching deeper high-temperature aquifers with the feasible technological solution in drilling while reducing the cost is critical. In this proceeding update, we summarized our works on the thermodynamic modeling of the AGS with its deployments horizontally and inclinedly. Through the analytical methodologies and sensitivity analysis, the horizontal and inclined well systems can provide stable heat energy but limiting by rock thermal conductivity, wellbore length and circulation rate. Detailed sensitivity analysis with consideration of multilateral wellbores interference are conducted to fully understand the AGS heat harvesting performance. In addition, the induced convective heat flow in the near-wellbore region and regional underground water flow are also discussed in this study. The results of the study could help to provide a better understanding of the thermodynamics of the AGS using horizontal and inclined well applications.

1. INTRODUCTION

The International Energy Agency (IEA) has presented a plan for various sectors to achieve net-zero emissions by 2050, which involves producing 90% of electricity from renewable sources such as wind, solar, hydro, bioenergy, and geothermal energy (IEA, 2021). This will require a significant investment in renewable generation and upgrading the electricity grid. However, renewable sources of energy like solar and wind are intermittent and not easily controllable (EIA, 2014; Kilpatrick, 2017; CER 2018). For example, solar power is less reliable in higher latitudes due to lower sunlight levels, and wind power can be disrupted by blade icing in winter. This makes it important to also develop dispatchable renewables like geothermal energy to ensure a stable supply of renewable electricity. In addition to electricity, geothermal energy can also be used as a heat source for buildings through the use of heat pumps. Canada, like many other countries, has committed to achieving net-zero emissions by 2050 (GC, 2021). While Canada has already made progress in using renewable resources (GC, 2022), there are still many challenges to meeting this goal. Geothermal energy could be a potential source of clean, stable, and dispatchable baseload energy for both electricity generation and district heating in Canada. In particular, geothermal resources of all types are important for Canada's clean energy supply (Grasby et al., 2011) as 80% of household energy in the country is used for space heating.

The Advanced Geothermal System (AGS), also known as closed-loop geothermal energy production technology, has gained much capital, advertising, and academic interest for its application in deep, high enthalpy systems for producing electric power (Yuan et al., 2021; Ghavidel et al., 2021; Beckers et al., 2022). This technology has been extensively applied to shallow underground systems, whether in the soil or water ponds, to produce/store energy for space heating or cooling (Zhang et al., 2019). Scientific and technical challenges prevent its implementation in deeper systems, such as difficulties in drilling, significant cost increases, resource assessment, and complex thermodynamic modeling. The common configurations of the closed-loop system are coaxial or single "U-loop" wellbore systems, or multiple wellbore U-loop systems (Shao et al., 2016). The U-loop system produces more heat theoretically by using the configuration of a vertical injection well and a vertical production well connected by a horizontal wellbore heat exchanger at the lower ends of the two. This AGS has many unique advantages over conventional geothermal technologies and enhanced geothermal system (EGS). The system can be installed where there are good reservoir temperature and rock thermal conductivity, without the need for suitable porosity, permeability and high fluid flow rates (Yuan, 2021). Therefore, it eliminates most risks of exploration including finding a permeable zone and water in place. Moreover, the working fluid—which can also be optimized for its thermal conductivity properties (e.g., CO₂)—is circulated in a closed-loop process system where there is no communication with reservoir fluids, which reduces the contaminations of the water system (Morales-Simfors and Bundschuh, 2022) and the level of corrosion in the pipe system (Faes et al., 2019; Karlsdottir, 2021). Although low rock thermal diffusivity (Kämmlein and Stollhofen, 2019; Yuan et al., 2021) limits the overall heat recovery efficiency, as compared to other geothermal technologies, due to the heat conduction being the main heat harvesting mechanism, it gains a longer heat production lifespan, which is another advantage over the traditional geothermal energy production methods.

The AGS has inherent challenges, however. Long horizontal wellbore and multilateral wellbore completions lead to significant drilling costs (Beckers et al., 2022), in addition to various technical challenges in horizontal wellbores connections (Eavor Technologies, 2022). However, with the improving development of drilling technology, the cost could be reduced and the technical difficulties could be overcome (Tessier et al., 2006); when the capital expenditures remain under control, the AGS will work in high geothermal gradient areas such as Turkey, Iceland, New Zealand and the Pacific ring of fire. The application to conduction-dominated systems such as sedimentary basins can be advanced by targeting well-defined, high temperature rock and higher thermal conductivity

layers (Yuan et al., 2021). While the reservoir temperature increases with increasing depth, the rock thermal conductivity is mainly a function of rock lithology, and may vary with depth.

An AGS using an inclined multilateral well configuration was proposed to improve the heat production output and reduce drilling costs (Eavor Technologies, 2022). Compared to the horizontal lateral wellbore design, the inclined well system can target a higher temperature reservoir. On the drilling and completion side, the inclined well system can place the vertical injection well and production well in the same area, thus reducing the cost of surface facilities. In addition, the inclined lateral well has fewer technical challenges in wellbore connections in the subsurface. In this proceeding update, the conceptional geological model of AGS is firstly introduced, as well as the major theoretical considerations and mathematical governing equations. Then, the analytical method strategy will be briefly described. Third, feature results of AGS system using horizontal and inclined wellbores are discussed with sensitivity analysis on key parameters. At last, the induced convective heat flow and the effect of underground water flow are discussed to expand the research of the heat harvesting performance of AGS.

2. PHYSICAL MODEL AND GOVERNING EQUATION

2.1 Reservoir and well configurations

A U-loop system features a horizontal well connecting injection and production wells 1-5 km apart (Fig. 1a), while an inclined well system is a fork-like design where the horizontal wellbore is split into two equal parts and the production and injection wells are close and inclined at angle θ to maximize depth (Fig. 1b). The fluid circulation and heat production are the same as in a closed-loop U-loop system.

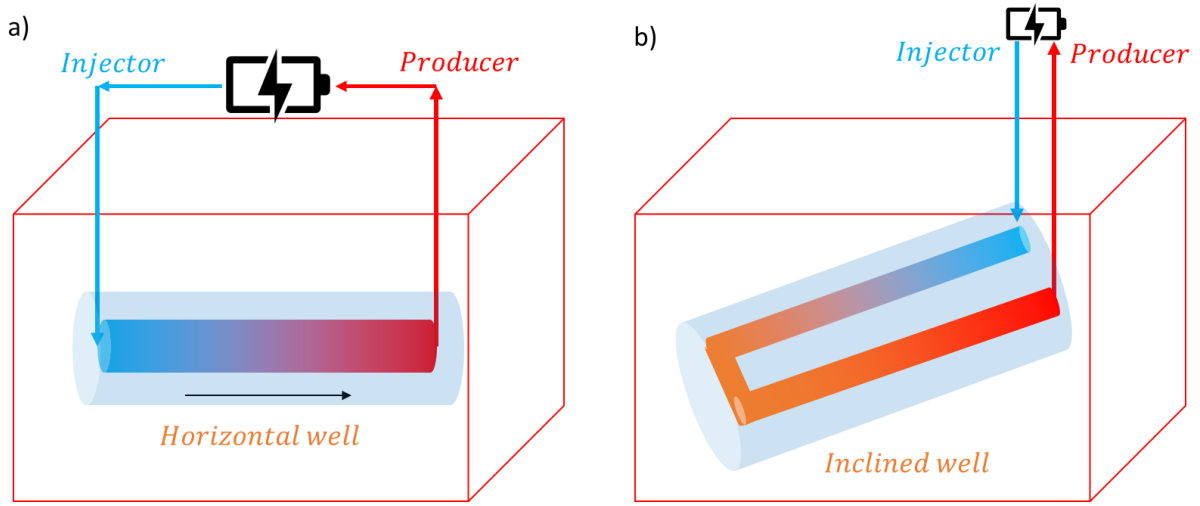


Figure 1. a) Schematic diagram of the traditional AGS using the horizontal well system; b) Schematic diagram of a new AGS using the inclined well configuration. Colours represent wellbore temperatures ranging from cold (blue) to hot (red). Revised from Yuan et al., 2021.

2.2 Modeling Assumptions

To analyze the thermodynamics of the inclined well system in AGS, the following assumptions have been made about the geological setting and heat transfer mechanisms in the system:

- 1) The source of heat energy is the Earth's geothermal heat flux with a constant geothermal gradient.
- 2) The heat transfer within the wellbore is simplified as a one-dimensional heat convection process as the wellbore diameter is much smaller than the reservoir.
- 3) The thermal resistance between the fluid and rock, including potential resistance from the steel tube wall, casing, and cement ring, is ignored.
- 4) The working fluid flow rate is constant throughout the thermal production period.
- 5) The thermal properties of the working fluid and the reservoir are considered constant and temperature-independent.

2.3 Governing equation

A previous mathematical model was created to assess the closed-loop geothermal system with multiple horizontal wells in high-enthalpy systems (Yuan et al., 2021). The energy transfer in the geothermal reservoir is determined by energy conservation:

$$\rho c \frac{\partial T}{\partial t} = \lambda \nabla^2 T \quad (1)$$

where ρ is the bulk density, c is the specific heat capacity, λ is the rock thermal conductivity, T is the rock temperature, and t is the time. The rock domain is subject to the initial temperature, $T_i(z)$ as a function of depth (z), and to transient heat flux from the rock to the wellbore, and to the constant geothermal heat flux.

The heat transfer in the inclined well yields the heat balance between convective heat transfer by the working fluid, and the conductive heat flow from the wellbore wall to the working fluid. Because of the length of the inclined lateral well, the depth of the toe and heel of the inclined section may have a significant difference. The uniform initial rock temperature of the major heat reservoir layer in regular closed-loop system simulation (Ghavidel et al., 2021; Yuan et al., 2021; Beckers et al., 2022) is no longer a valid assumption in this inclined well system. The geothermal gradient needs to be considered in the mathematical model. For example, in a geothermal reservoir with a 50 °C/km geothermal gradient, the temperature difference of the surrounding rock between the toe and heel of a 2-km long inclined well could be 50 °C (dip angle = 30°), 70.71 °C (dip angle = 45°), or 86.6 °C (dip angle = 60°). The continuity equation of the energy conservation in the inclined well system can be written as below considering the geothermal gradient:

$$A\rho_f c_f \frac{\partial T(x,t)}{\partial t} = -vA\rho_f c_f \left[\frac{\partial T(x,t)}{\partial x} - a \cdot \sin\theta \right] + q_c(x,t) \quad (2)$$

where A is the cross-section area of the wellbore, $\rho_f c_f$ is the volumetric heat capacity of the working fluid, a is the geothermal gradient, θ is the dip angle of the incline wellbore, v is the flowing velocity of the working fluid, q_c is the conductive heat flux from rock to the wellbore. The heat flux between hot rock and the wall of the wellbore can be calculated using analytical methods (Yuan et al., 2021).

3. METHODOLOGY

3.1 Vertical wellbores.

Yuan et al (2021) presented two analytical techniques without the use of meshes for modeling the thermodynamics of a closed-loop geothermal system. Duhamel's convolution theory was utilized to understand the relationship between the transient temperature and heat flux in the wellbore. This method is appropriate for a single wellbore system like the vertical injection and production well in an advanced geothermal system. The transient temperature T_v , K, at the end of the vertical wellbore in Laplace domain can be expressed as below:

$$\bar{T}_v = \frac{(T_r - T_{inlet})}{s} \cdot \exp\left(-\frac{sD}{Av\rho_f c_f} \cdot \bar{q}_{cu} - s \cdot \frac{D}{v}\right) \quad (3)$$

where, T_{inlet} is the temperature of working fluids at the beginning of lateral wellbore, K; T_r , reservoir temperature (K); D is length of the vertical wellbore which is also the depth of the target wellbore, m; $\rho_f c_f$ is the volumetric heat capacity of the working fluid; q_{cu} is the conductive heat flux under unit temperature difference calculated from the standard source and sink functions; and s signifies the Laplace transform parameter; symbols with “ $\bar{}$ ” means parameters in Laplace domain. The temperature at the end of the vertical injection wellbore will be used as the input to the calculation for the inclined wellbores system. Similarly, the temperature at the end of the inclined wellbore will also be used as the input to the calculation for the vertical production wellbore.

3.2 Horizontal and Inclined wellbores.

The Natural Coupling Method (NCM) was first proposed to solve the multilateral wellbore configurations modeling in AGS. Transient heat flow from the rock to the wall of the wellbore can be accurately calculated. The general philosophy is to divide the whole system into two sub-systems which share the same conductive heat flux and temperature at the contact faces (Fig.2). The inclined wellbore is divided into many sub-segments to calculate heat flux and temperature in each segment. Sub-system #1 can be seen a standard 3D model with a line heat sink in the center of the system, which can be described by integral instantaneous source and sink functions. Sub-system #2 is a 1 D wellbore model composed of multiple sub-segments, which can be described by heat conservation equations with connection at two endpoints of each segment.

The impact of multiple wells on each other can be accounted for using the superposition principle. However, the NCM only considers horizontal wells completed in a horizontal plane with uniform initial temperatures in the model. The inclined well system has a long length, leading to significant depth differences and temperature differences between the heel and toe of the well (Fig. 1b). To model the inclined well system, a coordinate rotation has been applied to transform the horizontal well system into the inclined well system in the mathematical model, creating three new axes:

$$x = Sc(x' \cos \theta - z' \sin \theta) + \Delta x \quad (4)$$

$$y = y' \quad (5)$$

$$z = Sc(x' \sin \theta + z' \cos \theta) + \Delta z \quad (6)$$

where Sc is the scale, θ is the angle of rotation, $\Delta x, \Delta z$ are the transition in x and z axis, the superscript “ $'$ ” denotes the coordinates in original system.

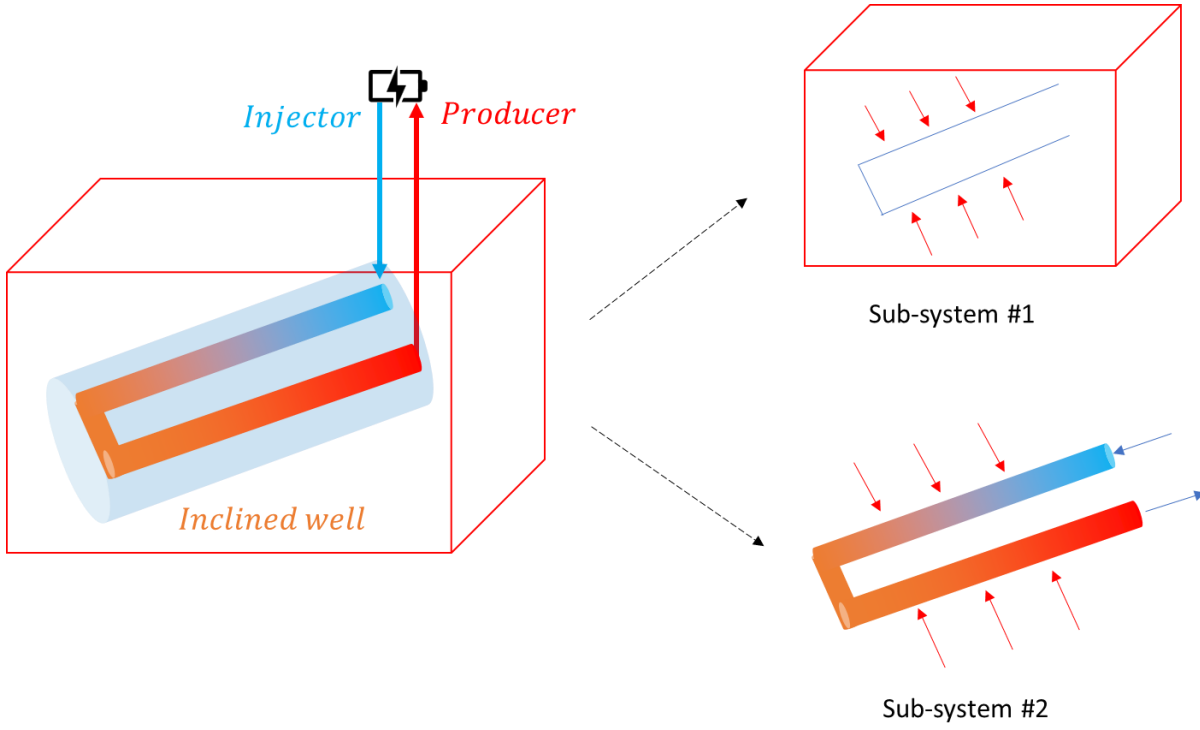


Figure 2 Illustration of the Natural Coupling Method.

The inclined descending and ascending wellbores are divided into segments (Fig. 3) for accurate calculation of heat influx using source and sink functions applied in heat transfer in porous media. In the study, the temperature change from the i^{th} segment of the descending wellbore and the j^{th} segment of the ascending wellbore can be represented as:

$$\Delta T^i = \int_0^t \frac{q^i(\tau)}{\rho c} \cdot T_{sx}^i(t-\tau) T_{sy}^i(t-\tau) T_{sz}^i(t-\tau) d\tau \quad (7)$$

$$\Delta T^j = \int_0^t \frac{q^j(\tau)}{\rho c} \cdot T_{sx}^j(t-\tau) T_{sy}^j(t-\tau) T_{sz}^j(t-\tau) d\tau \quad (8)$$

where $q^i(\tau)$ and $q^j(\tau)$ are the instantaneous transient heat influx from the rock to the i^{th} and j^{th} segments; the $T_{sx}^i(t-\tau)$, $T_{sy}^i(t-\tau)$, $T_{sz}^i(t-\tau)$, $T_{sx}^j(t-\tau)$, $T_{sy}^j(t-\tau)$, $T_{sz}^j(t-\tau)$ are source/sink functions of the i^{th} and j^{th} segments in x, y, z directions which can be expressed using the formulas in NCM (Yuan et al., 2021). By using the superposition principle, the temperature change at any point can be expressed as a form of summations of all the inclined wellbore segments:

$$\begin{aligned} \Delta T(x, y, z, t) = & \sum_{i=1}^{N_L} \int_0^t \frac{q^i(\tau)}{\rho c} \cdot T_{sx}^i(t-\tau) T_{sy}^i(t-\tau) T_{sz}^i(t-\tau) d\tau \\ & + \sum_{j=1}^{N_L} \int_0^t \frac{q^j(\tau)}{\rho c} \cdot T_{sx}^j(t-\tau) T_{sy}^j(t-\tau) T_{sz}^j(t-\tau) d\tau \end{aligned} \quad (9)$$

The temperature change calculated by the source and sink functions will then be matched with results from the solutions (Yuan et al., 2021) from Eq. 2 with consideration of the thermal gradient. The temperature of any point in k^{th} ($k \in [1, 2N_L]$) segment of the inclined lateral wellbore (including descending and ascending wellbores) can be calculated by the following equations:

$$\begin{aligned} \overline{\Delta T^k(x)} = & \overline{\Delta T_{x=0}^k} \cdot e^{-\frac{s}{v}x} + \left(1 - e^{-\frac{s}{v}x}\right) \left(\frac{\overline{q^k}}{sL_{seg}A\rho_f c_f} + \frac{asin\theta}{s^2}\right), 0 \leq x \leq L_{seg} \\ \overline{\Delta T_{x=0}^k} = & \overline{\Delta T_{x=L_{seg}}^{k-1}} \\ \overline{\Delta T_{x=L_{seg}}^k} = & \overline{\Delta T_{x=0}^{k+1}} \\ \overline{\Delta T_{x=0}^1} = & \frac{T_r}{s} - \overline{T_v} \end{aligned} \quad (10)$$

where L_{seg} is the length of each segment of the inclined wellbore; x is the location of any point in this segment. As a result, the transient heat influx values, $\overline{q^k}$, can be solved by Gaussian elimination for the matrix formed by Eq. 9 and Eq. 10. The numerical calculations of Laplace transformation, matrix solver, and time domain inverse process are coded in Microsoft® Visual Studio C++ environment. The final solutions are then be inversed to real time domain by applying the Laplace transformation Stehfest inverse algorithm (Stehfest, 1970).

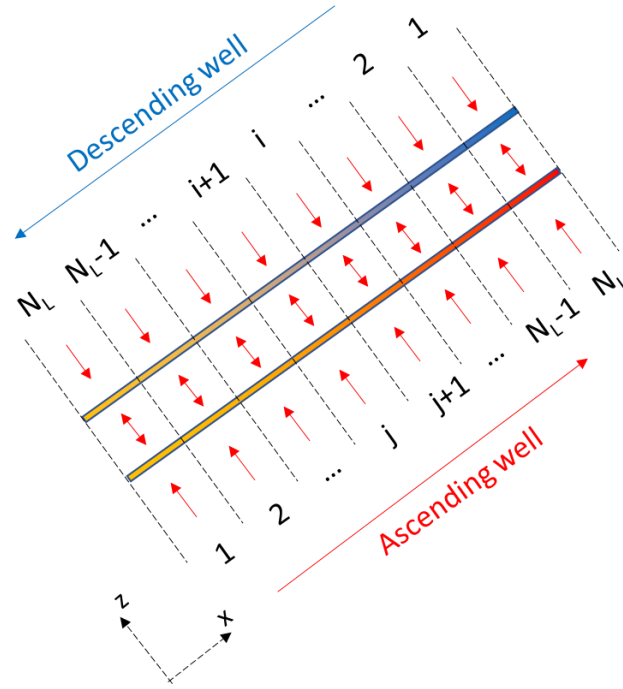


Figure 3. Schematic diagram of N_L segments divided from each inclined wellbore. Revised from Yuan et al., 2023.

4. HEAT PRODUCTION PERFORMANCE

4.1 Geological setting of the example case.

A geological model of a sedimentary basin underlain by igneous basement used for this case study is shown in Figure 4a. Zone 1 represents the sedimentary basin rock, where the vertical injection and production well are installed and the rock thermal conductivity is relatively low. Zone 2 is the targeted geothermal reservoir in the Crystalline basement with desirable temperatures and high thermal conductivity. The top of Zone 2 is located at 3 km depth, with an initial reservoir temperature of 150 °C at 3 km. Other related reservoir and well parameters are listed in Table 1. Two inclined lateral wellbores are then drilled into Zone 2 at an angle of θ . The two laterals are connected at the far end of the wells to form a closed loop. The two lateral inclined wells are 20 m apart, and have a length of 2 km with a 45° angle deviation from vertical at 3 km depth. This well design makes the maximum depth 4.414 km with a 218 °C initial reservoir temperature. In order to have a better understanding of the heat production enhancement by the inclined system, a closed-loop with the horizontal lateral well system is set up as the comparison case (Fig. 4b). The horizontal wellbore is set in Zone 2 with homogeneous reservoir temperature at 150 °C. Since the lateral length of the inclined system is 2 km, the lateral length of the horizontal well system is 4 km. Other parameters in the horizontal well system are the same as the inclined well system listed in Table 1.

Table 1. Parameters of reservoir and the closed loop well system used in the modelled case.

Zone	Parameter	Symbol	Value	Unit
Zone 1	Surface temperature	T_s	5	°C
	Temperature at 3 km depth	T_r	150	°C
	Temperature of the inlet at the injection well	T_{inlet}	60	°C
	Depth at bottom of Zone 1	D	3	km
	Rock thermal conductivity of Zone 1	λ_1	2.0	W/m/K
	Inner diameter of the vertical wellbore	d_v	0.21	m
	Density of the rock in Zone 1	ρ_{r1}	2500	kg/m ³
	Specific heat capacity of the rock in Zone 1	c_{r1}	1100	J/K/kg
Zone 2	Length lateral	L	2	km
	Geothermal gradient	α	0.0483	°C/m
	Temperature at the top of the inclined wellbore	T_{2t}	150	°C

	Inner diameter lateral	d_l	0.156	m
	Distance between a pair of laterals	h	20	m
	Inclined dip angle	θ	45	°
	Density of the rock in Zone 2	ρ_{r2}	2600	kg/m ³
	Specific heat capacity of the rock in Zone 2	c_{r2}	1100	J/K/kg
	Segment length used in Natural Coupling Method	L_{seg}	200	m
	Working fluid circulating flow rate	q_f	20	m ³ /hr
	Density of the working fluid	ρ_f	1000	kg/m ³
	Specific heat capacity of the working fluid	c_f	4180	J/K/kg

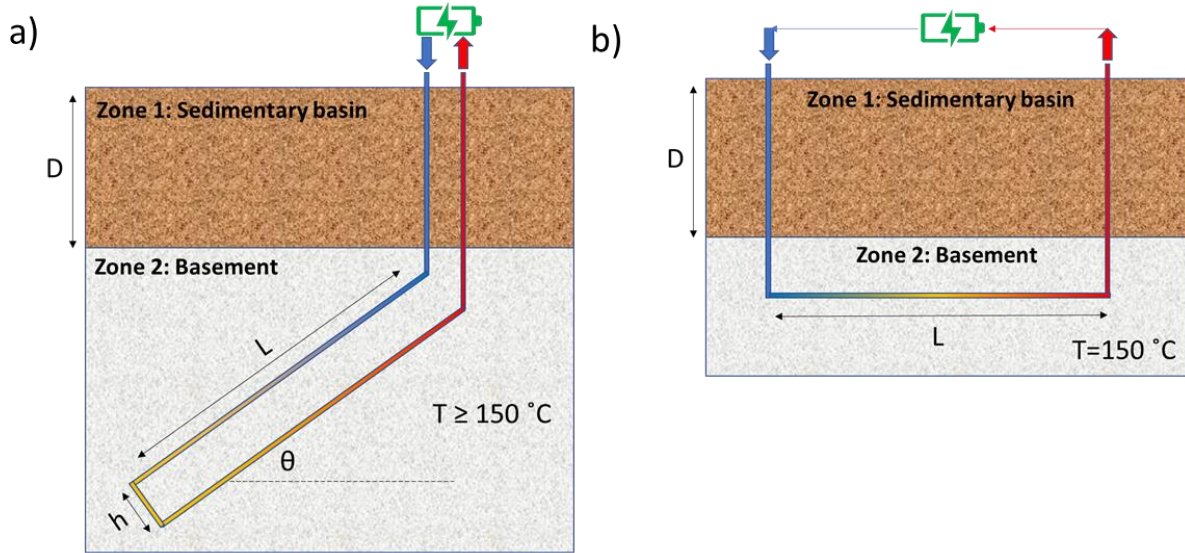


Figure 4. Schematic diagram of the AGS using the a) inclined well system or b) horizontal well system. Key geometry parameters are shown in the figure. Colours represent working fluid temperatures ranging from cold (blue) to hot (red). The battery symbol reflects end heat usage (direct heat use and/or power generation). Revised from Yuan et al., 2023.

4.2 Heat production performance of the multilateral wellbore system

Figure 5 shows the 3D visualization of the reservoir temperature at the end of 30 years by a 5-lateral AGS system. A cubic volume near the inclined wellbores is chosen to show the temperature profile (Fig. 5 left). The blue line represents the vertical injection wellbore and the red line represents the vertical production wellbore. The right panel of Figure 5 shows the view of the plane that the descending wellbores lie in. Figure 6 shows the 2D birds-eye view of the temperature distributions of the descending wellbore (Fig. 6 upper) and ascending wellbore (Fig. 6 lower) planes. The flow direction in the descending wellbore is from right to left, while the direction in the ascending wellbore is from left to right. The inclined 10 wellbores can be clearly identified by the blue colour, which means the temperatures of the working fluid in wellbores are lower than that of the surrounding reservoir. The temperature increase along the working fluid flow direction can also be identified. Because the spacing distance of the well pair is only 25 m, the reservoir temperature drop area has been merged together, which means that wellbore interference has occurred. Three cross-section views of the temperature distribution at three different locations of the near wellbore reservoir are plotted in Figure 7. The oval shape of the temperature drawdown area is clearly shown by the light blue color area. The five upper descending inclined lateral wellbore and five lower ascending inclined lateral wellbores can also be identified. Because the upper and lower wellbores only have 20 m spacing, the light blue area between two sets of wells represent the wellbore interference effect.

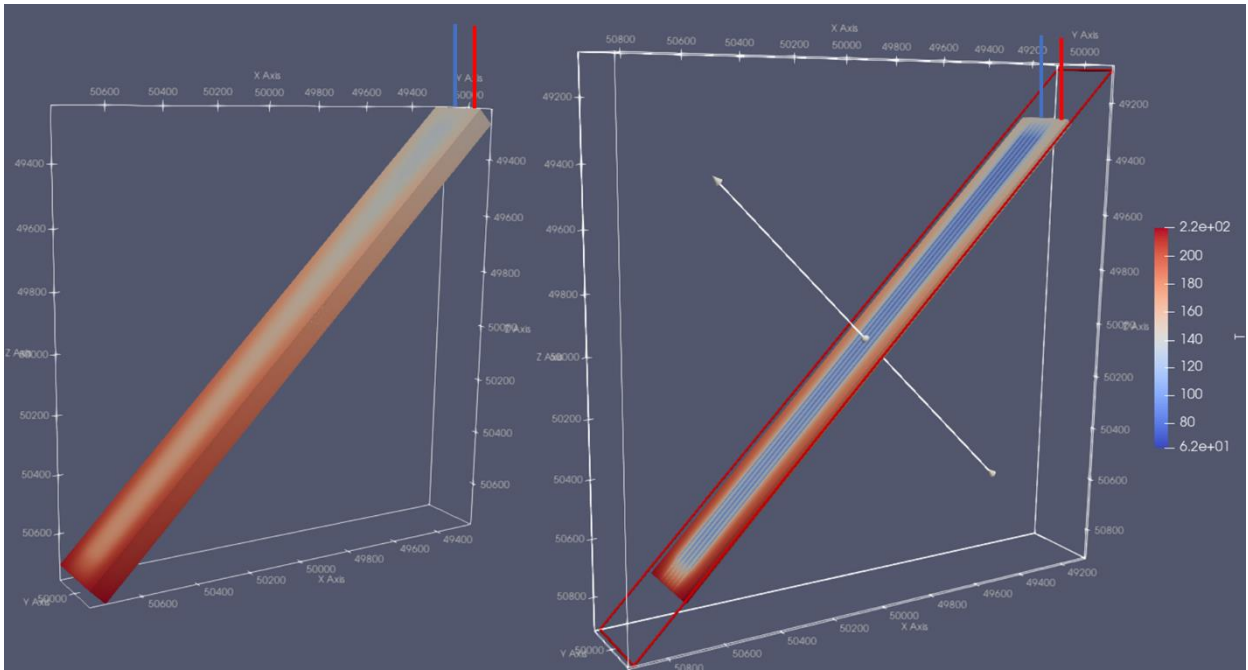


Figure 5. Temperature distribution of the reservoir (left) and cutting view (right) of the plane where the descending wellbores are lying in at the end of 30 years. Colours represent the temperatures ranging from cold (blue) to hot (red).

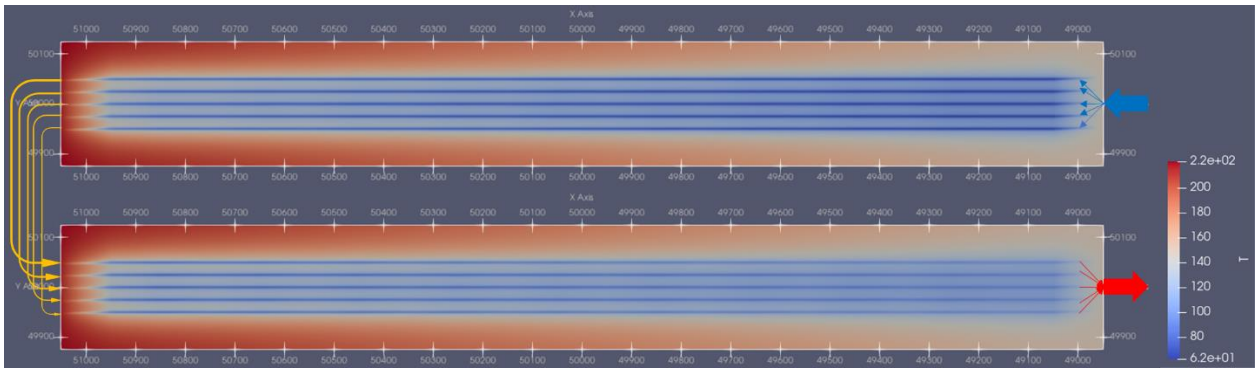


Figure 6. Temperature distribution of the reservoir at the planes of descending (upper) and ascending (lower) wellbores at the end of 30 years. Colours represent the temperatures ranging from cold (blue) to hot (red).

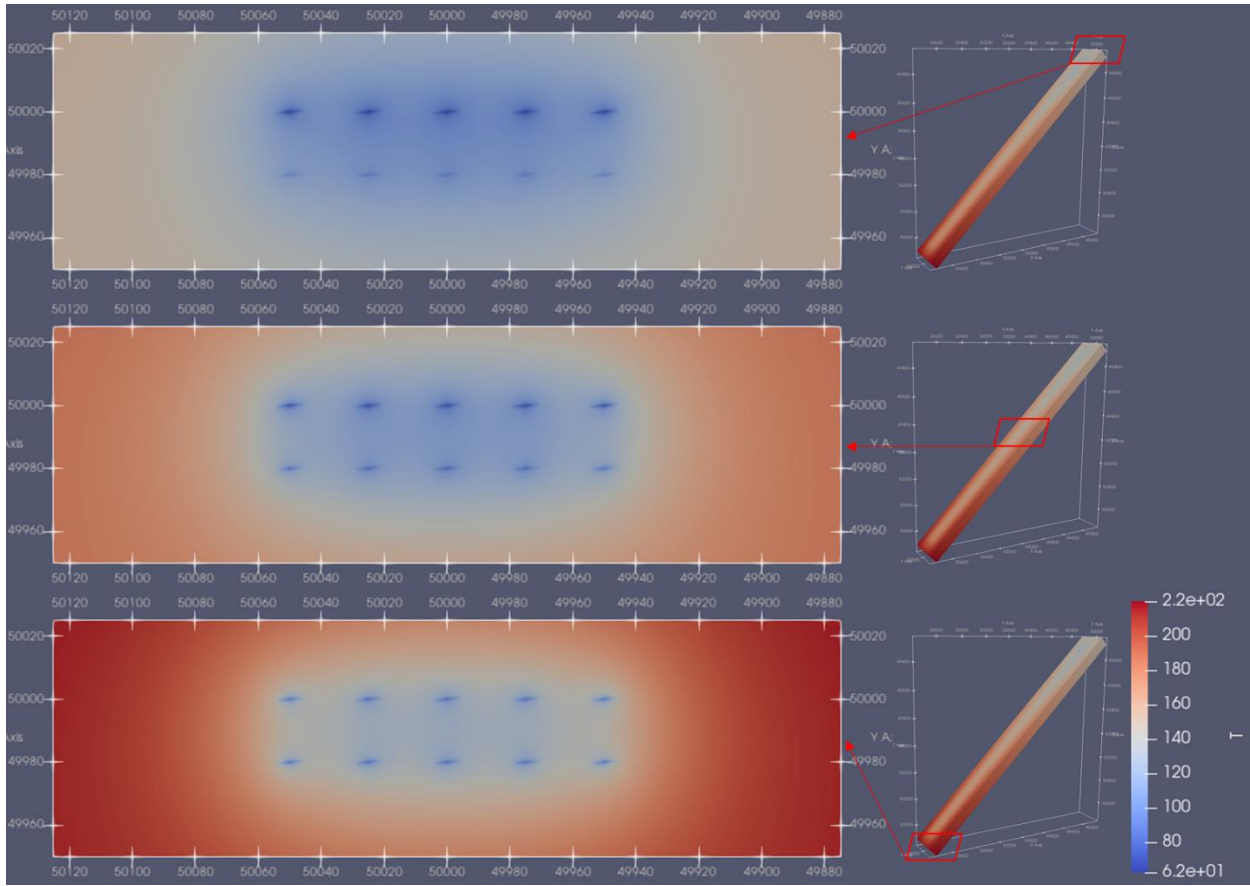


Figure 7. Temperature distribution of the reservoir at the three cross-sections (upper, middle, and lower) of the reservoir at the end of 30 years. Colours represent the temperatures ranging from cold (blue) to hot (red).

Four different numbers of multilateral wellbores are studied to investigate the multiple wellbore system heat production performance. The outlet temperatures over 30 years are plotted in Figure 8a. The result of the single lateral case is also plotted in black colour as the baseline. They have the same 20 m spacing distance between the descending and ascending wellbores (h), 25 m wellbore pair spacing distance (W), 45° inclined angle (θ), and 2 km long single lateral length (L). A larger number of laterals will provide a higher outlet temperature by reducing the heat loss in the vertical production wellbore section because of the higher flow rate in the vertical wellbore. However, severe wellbore interference will significantly reduce the heat extraction ability later in the production period. The single lateral case has the highest outlet temperature at later production periods. As minimizing the wellbore interference for multilateral wellbore completion is critical to the success of the whole well pad facility, more sensitivity analyses of wellbore interference effect are examined in the next section.

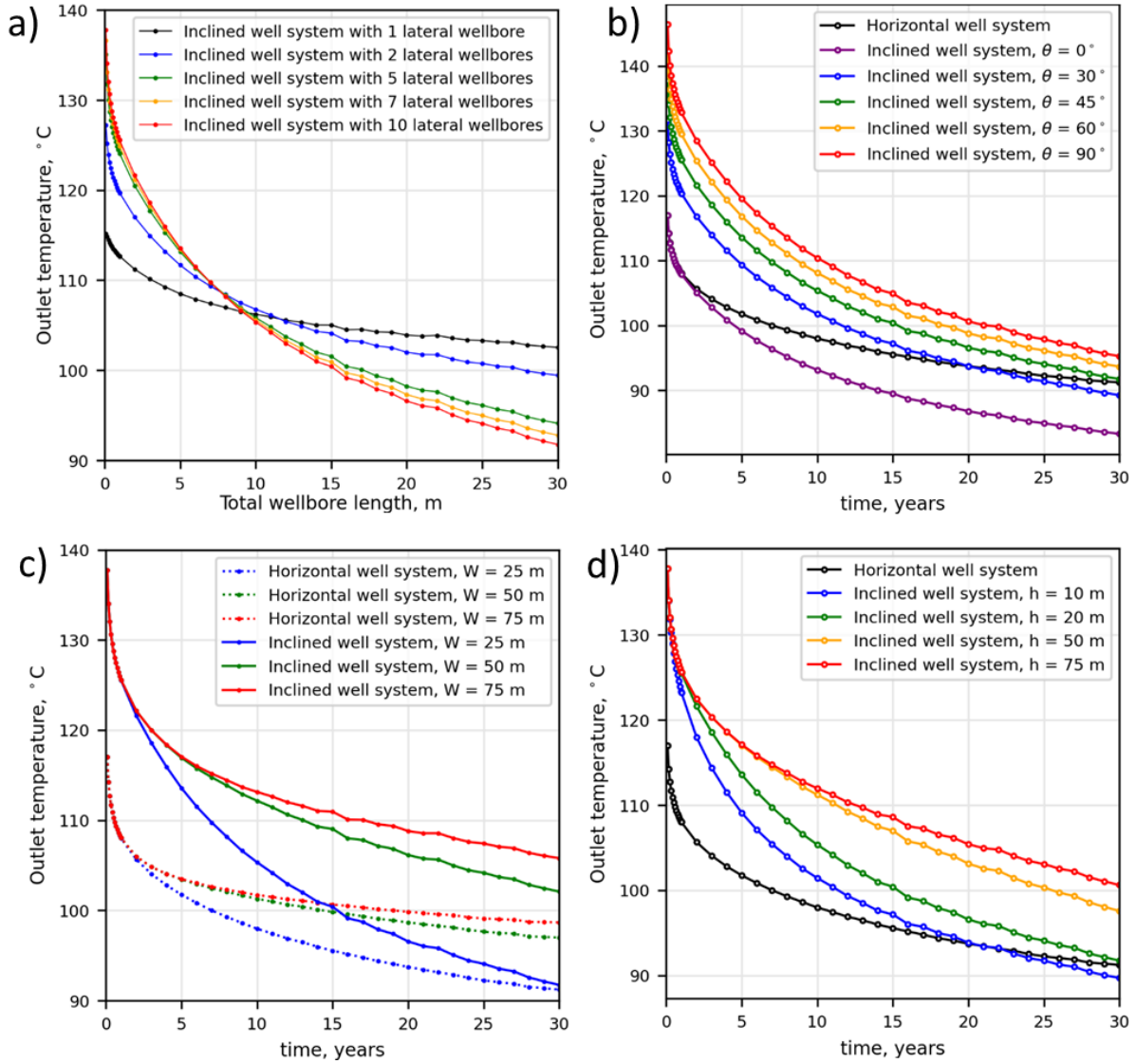


Figure 8. Outlet temperature profiles over 30 years under various numbers of the inclined laterals. Revised from Yuan et al., 2023.

The previous section shows the important concerns about the wellbore interference issue among the dense wellbores setup in the AGS with an inclined well system. This interference will significantly affect the overall performance, resulting in lower heat production than the traditional AGS horizontal well system. A 10-lateral AGS system is used to analyze the wellbore interference effect. Figure 8b plots the results of the outlet temperature under various dip angles in the 10-laterals case with fixed h of 20 m and W of 25 m. High angle wellbores help the lateral reach a higher temperature reservoir under the same lateral length. However, because of the close distance between multilateral wellbores, the cases with over 45° inclined angles could have better outlet temperature over 30 years than the horizontal well system. In order to study the optimum options to reduce the wellbore interference effect, other sensitive analysis on the spacing distance between the wellbores needs to be examined.

Two types of wellbore spacing will affect the wellbore interference effect. One is the distance between the nearby parallel well pairs, or horizontal spacing (W). The sensitive study of this spacing distance is shown in Figure 8c. The dotted lines in Figure 8c are the results of corresponding cases by the horizontal well system. The same colour represents the same spacing distance. The best heat production result in both lateral systems is provided by 75 m spacing. However, considering the inclined well system will still have the internal interference effect by the descending and ascending wellbores, the outlet temperature by the inclined well system decreases faster and may be lower than the horizontal well system (25 m spacing cases). The outlet temperature difference between 50 and 75 m spacing distance is not obvious. As a result, at least 50 m well pair spacing distance can help this system minimize the wellbore interference in this direction. Another interference cause is the distance (h) between the descending and ascending inclined lateral wellbores. Figure 8d shows that $h > 50$ m could significantly increase the outlet temperature of the whole system by reducing the well pair internal interference effect. As a result, at least 50 m spacing distance between any two wellbores need to be considered in the well pad design.

In order to calculate the ideal energy production performance of the multilateral inclined wellbore system of 10 wells in AGS, a 75 m spacing is applied to both well pairs, and the descending and ascending wellbores. A 2 km long inclined lateral is used in the system and a 45° dip angle is applied in the drilling design. The inclined well system of AGS can provide over 15 MW_{th} heat energy (125 °C production temperature) in the first year and generate over 12 MW_{th} heat energy (112 °C production temperature) over the

rest of 30 years of operation (Fig. 9). Compared with the same set of the horizontal well system, 3 MW_{th} more heat energy can be generated by this inclined well system. Almost 1000 GWh_{th} more heat energy could be recovered at the end of 30 years by the inclined well system than conventional horizontal AGS system.

Considering its application in igneous rock formation, the outlet temperature and flow rate could meet the need for electricity power generation and has its own advantages compared to other geothermal energy production technologies. We have restricted our assessment to the thermodynamic viability of this technology and the economic aspects (mostly related to drilling costs) are not considered in this study. For commercial consideration, there should be a balance among the circulation flow rate, length of the lateral, wellbore inclined angle, distance between pairs and paired wells, and other parameters related to the surface utilization. Optimization could find the optimal pairing for those parameters. In addition, the inclined wellbore drilling to a deeper reservoir has its own technical challenges and extra capital cost. Overall, the AGS using an inclined well system would generate more energy, and reduce the challenges of drilling, as compared to a traditional AGS system. The economic and drilling aspects should be examined to study its feasibility in commercial heat production.

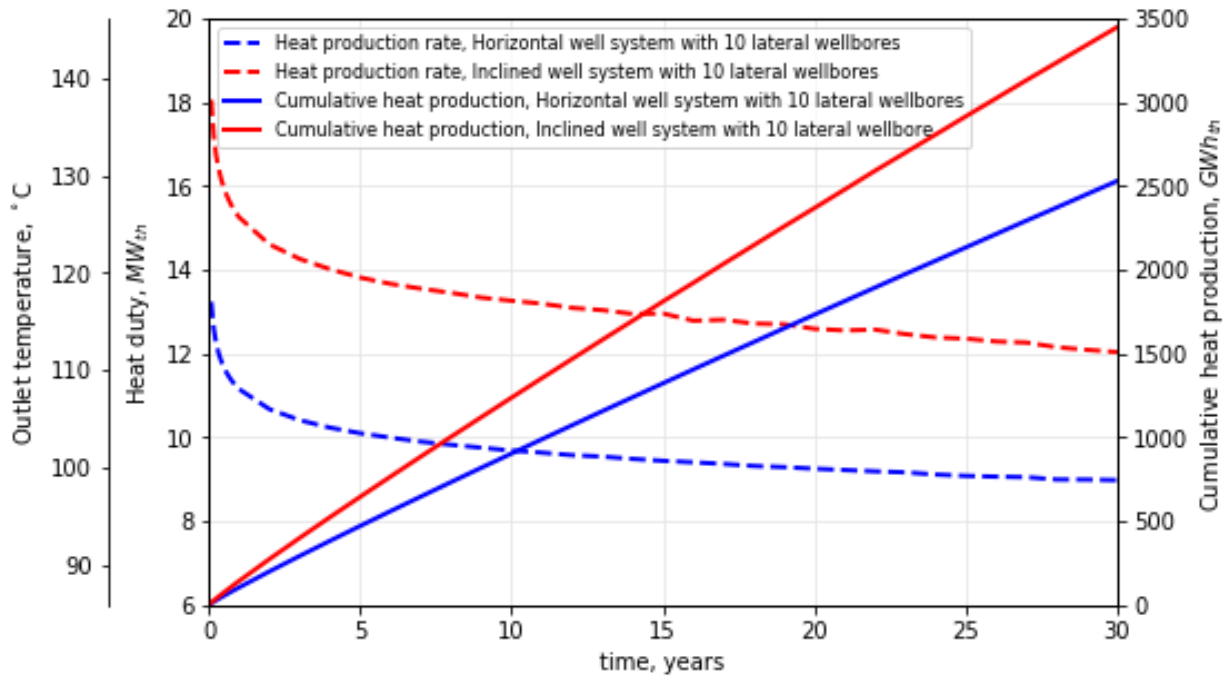


Figure 9. Heat duty and cumulative thermal production profiles over 30 years of 10-laterals case by the AGS using the inclined well system (red) and the horizontal well system (blue).

5. INDUCED CONVECTIVE HEAT FLOW

When AGS is deployed in some high permeable or vertically fractured rock formations like fractured igneous basement reservoir, the impact of induced convective flow due to density difference needs to be considered in heat production performance analysis or equivalent thermal conductivity calculation. The induced density-driven heat convection contains multiple physical processes. The cold working fluid flows within a sealed horizontal pipe completed in a high temperature formation with good thermal conductivity. The heat is transferred through the wellbore wall to the working fluid inside, and then the heated fluid is produced out through vertical wellbore. Due to the large fluid velocity inside the pipe, heat convection process dominates the heat transfer performance along the fluid flow direction. Previous researches usually assume pure heat conduction mechanism outside the pipe, where the heat is transferred from higher temperature bulk body to lower ones, with no fluid flow inside the formation considered thus leading to a pure conductive heat process without any convective flow involved. However, in reality the fluid in the reservoir nearby wellbore will experience heat loss to the pipe, causing its density to increase and certain degree of thermal shrinking will happen too. Fig. 10a illustrates that a fluid element nearby the pipe is losing its heat, and then its temperature decreases with a density increase and volume shrinkage, then a corresponding convective fluid flow will occur. Due to the physics of heat transfer diffusion process, this kind of induced density-driven convection flow will occur only in the near-wellbore region. The fluid near the pipe will firstly lose heat to wellbore and consequently cause a density increase and volume shrinkage. The density gradient generated will result in a downward flow. The left-over volume generated by the shrined volume will be occupied by higher temperature fluids coming from upward layer mainly, with supporting warmer fluid feeding from surrounding environment as well. The fluid in the lower position will then moving upward. The total process will form a natural density-driven convection flow process nearby the heat production pipe, which in general will enhance the heat transferred to closed-loop system (Fig. 10b). Except applied in hot dry rock, sedimentary basins usually have good permeability and porosity, as well as natural fractures or induced fractures near the wellbore. All these features will help enhance the induced density-driven convective flow process within the reservoir.

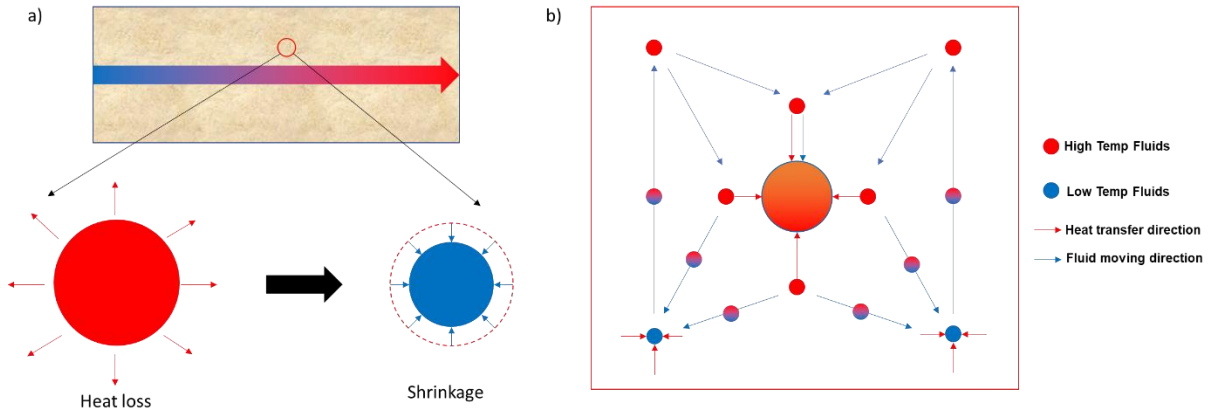


Figure 10 a) Illustration of a fluid element losing heat and causing a volume shrink; b) Illustration of the vertical section view of the induced density-driven heat convective flow.

The upper figures in Fig. 11 shows the pressure distribution and convection flow velocity streamline of the cases with the three different permeabilities at a time of 1 year. Because there are no conventional hydraulic source/sink in the system, the pressure level remains stable throughout the heat production period. Due to density change and fluid volume shrink, the induced density-driven convective flow occurs and the velocity streamline can be seen clearly to show the direction of the flow. The convective flow starts from the horizontal wellbore towards down below, and then it will flow upwards to form a circle due to the gradual phase warming up as it moves downwards. When the permeability increases, the velocity of streamline shows more intensely below the horizontal wellbore, representing significant induced natural convective flow. Three different permeabilities (10 mD, 1 D, 10 D) have been investigated in this 3D model to mimic three different vertical formation connectivity. The lower figures in Fig. 11 shows the velocity distribution and the streamline profiles. When permeability is 10 mD, the induced flow velocity is small and in the range of $e-10$ to $e-9$ m/s. The region near the wellbore has the most significant induced density-driven velocity, which denotes the significant temperature change in that area. When the permeability increases to 1 D, the velocity increase is not that much compared with the case with 10 mD permeability. When it comes to 10 D permeability case, the velocity increases largely to a range of $e-7$ to $e-6$ m/s.

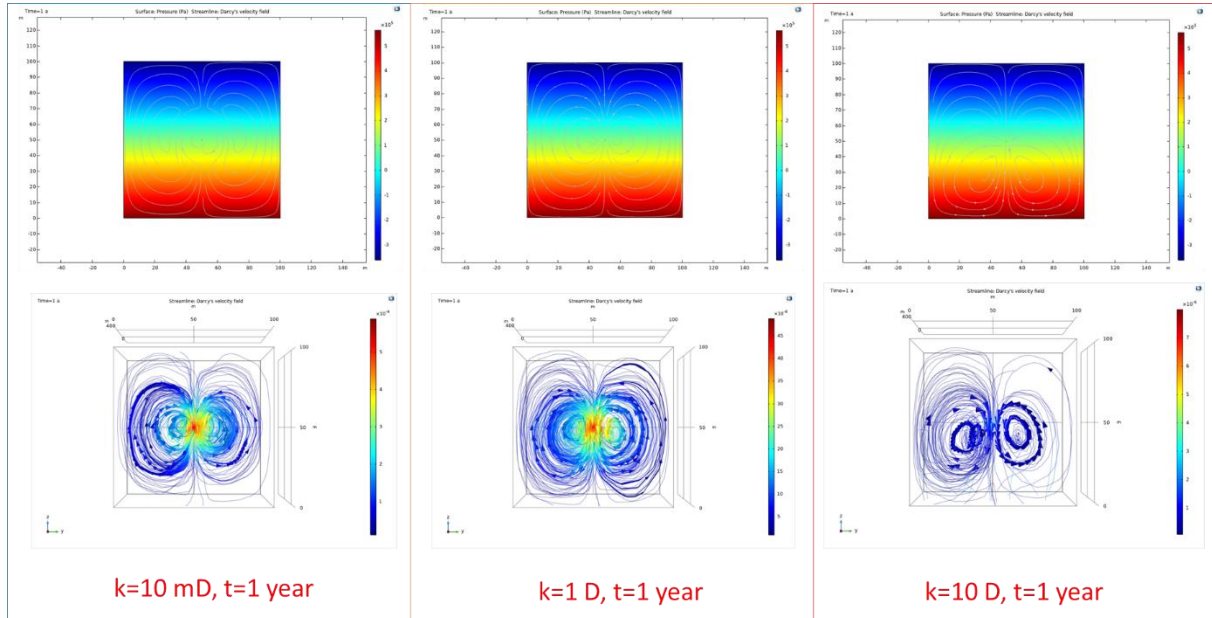


Figure 11 Pressure distribution and convection flow velocity streamline of the cases with the three different permeabilities at a time of 1 year.

6. UNDERGROUND WATER FLOW

The heat production performance could be enhanced by deploying AGS in formations with underground water flow. The impact of regional groundwater flow (or hydrothermal flow), particularly the focused flow along high permeable conduits or fracture/fault zones (presumably the thermal reservoir), on the production presents a knowledge gap in recoverable resource and production forecasting. In this numerical simulation study, the induced convective flow by gravity is neglected. Due to the existing regional groundwater flow, the effect by the induced convective flow by gravity is very limited in the overall heat transfer process. The forced heat convection plays the major role in heat convection process. A numerical model of the closed-loop system in a cuboid shape geothermal reservoir is generated and the geometries can be found in Figure 12. A 500 m long horizontal wellbore is located in the center of the reservoir. The initial temperature of the reservoir is 200 °C and the inlet cold water temperature is set at 60 °C.

The water flow velocity and direction of the underground water in the Meager Mountain, BC, Canada area are studied based on one hydrology study in 1979. By mathematical simulations, the most likely values for the regional underground water flow are 5×10^{-8} m/s in the horizontal direction in the basement rocks, 1×10^{-7} m/s for the vertical direction in the basement rock, 1×10^{-7} m/s for the volcanics and 7×10^{-7} m/s for the fault zone. 10 different cases are studied to learn how the underground flow affects the closed-loop geothermal energy production. Case #0 is the case without regional underground flow as the base comparison case. Case #1 to Case #5 are the cases which the flow direction is in pure x, y and z direction. The closed-loop flow direction is fixed in x axis direction in all cases. Case #6 to Case #10 are the cases which the flow has two directions. In general, the horizontal velocity is fixed at 5×10^{-8} m/s and the vertical velocity is fixed at 1×10^{-7} m/s. The detailed case descriptions are introduced in the following section.

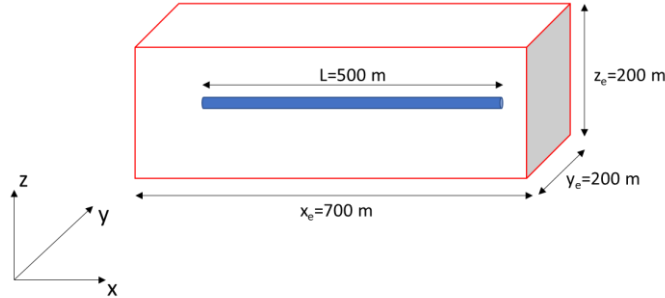





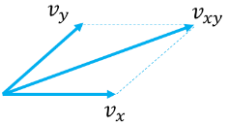
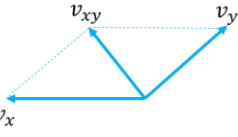
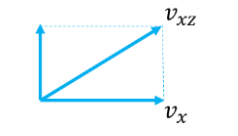
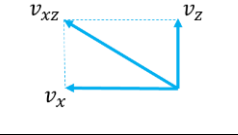
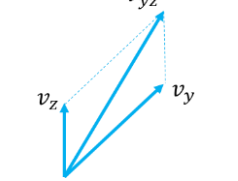


Figure 12 Schematic diagram of the numerical model setting.

Regional underground water flow. The water flow velocity and direction of the underground water in the Meager Mountain area are studied based on one hydrology study in 1979. By mathematical simulations, the most likely values for the regional underground water flow are 5×10^{-8} m/s in the horizontal direction in the basement rocks, 1×10^{-7} m/s for the vertical direction in the basement rock, 1×10^{-7} m/s for the volcanics and 7×10^{-7} m/s for the fault zone. 10 different cases are studied to learn how the underground flow affects the closed-loop geothermal energy production. Case #0 is the case without regional underground flow as the base comparison case. Case #1 to Case #5 are the cases which the flow direction is in pure x, y and z direction. The closed-loop flow direction is fixed in x axis direction in all cases. Case #6 to Case #10 are the cases which the flow has two directions. In general, the horizontal velocity is fixed at 5×10^{-8} m/s and the vertical velocity is fixed at 1×10^{-7} m/s. Detailed case descriptions are introduced in the following section.

Table 2 10 study cases velocity parameters and flow directions.

Flow direction	Case #	$v_x(m/s)$	$v_y(m/s)$	$v_z(m/s)$
N/A	0	0	0	0
	1	5×10^{-8}	0	0
	2	-5×10^{-8}	0	0
	3	0	5×10^{-8}	0
	4	0	0	1×10^{-7}
	5	0	0	7×10^{-7}

	6	3.535534×10^{-8}	3.535534×10^{-8}	0
	7	-3.535534×10^{-8}	3.535534×10^{-8}	0
	8	5×10^{-8}	0	1×10^{-7}
	9	-5×10^{-8}	0	1×10^{-7}
	10	0	5×10^{-8}	1×10^{-7}

The outlet temperatures over 30 years operation of 10 cases are plotted in Figure 13 with illustration of the velocity direction. The case of the circulating water direction inverting to the horizontal underground water flow direction has better heat production performance than the case with the same direction. For example, the outlet temperatures of Case #2 is higher than Case #1, but the difference is too small to be identified from the plot. Second, the case of the regional flow direction perpendicular to the horizontal wellbore has much higher production performance. That is because the underground flow has larger contact area with the horizontal wellbore and enhance the heat production. And higher flow velocity will contribute to higher outlet temperature. Case #5 has the highest flow velocity, and its outlet temperatures are highest.

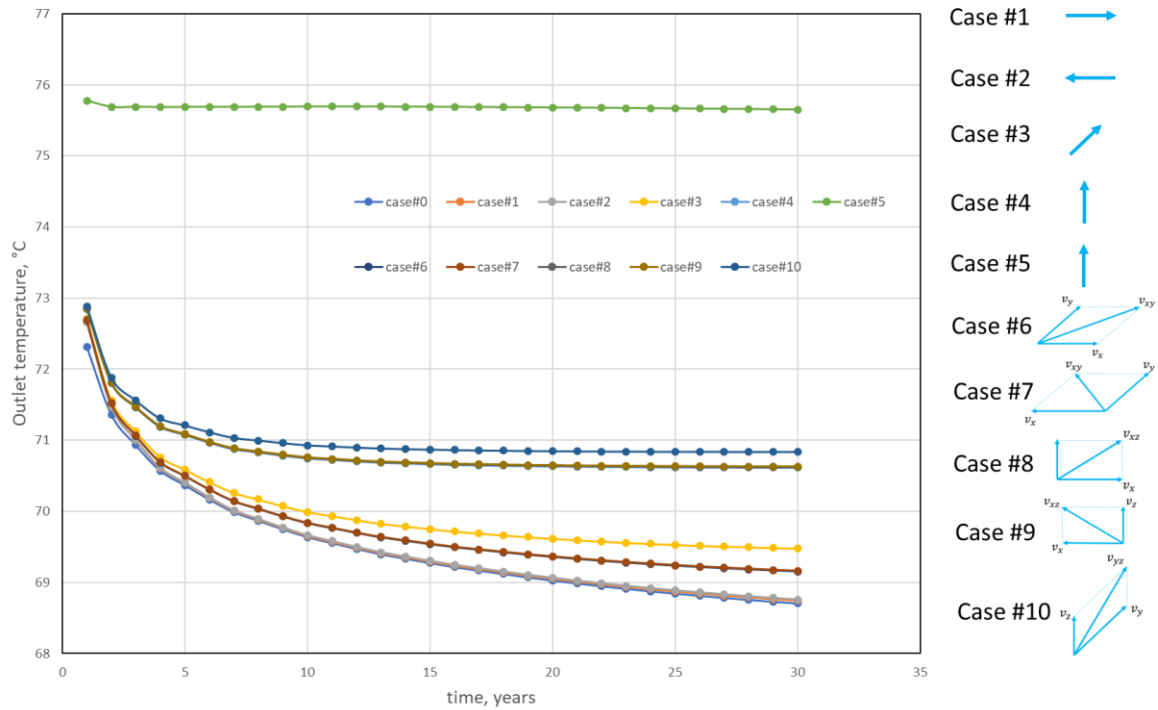


Figure 13 The outlet temperatures of the 10 cases over 30 year operation.

In order to further the study of the enhancement effect under various flow velocity, fixed flow direction is set to be perpendicular to the wellbore as shown in Figure 14. 10 different regional flow rates across 5 orders of magnitude are studied. The outlet temperature at the end of 30 years under various velocity values are plotted in Fig. 14. We can see that when the velocity is less than $1\text{e-}8$ m/s, the regional flow has limited enhancement effect on the closed-loop system. The thermodynamic enhancement by regional flow becomes significant when the velocity falls between $1\text{e-}8$ to $5\text{e-}6$ m/s. If the velocity is larger than $5\text{e-}6$ m/s, the regional flow will not provide more enhancement on the heat production performance.

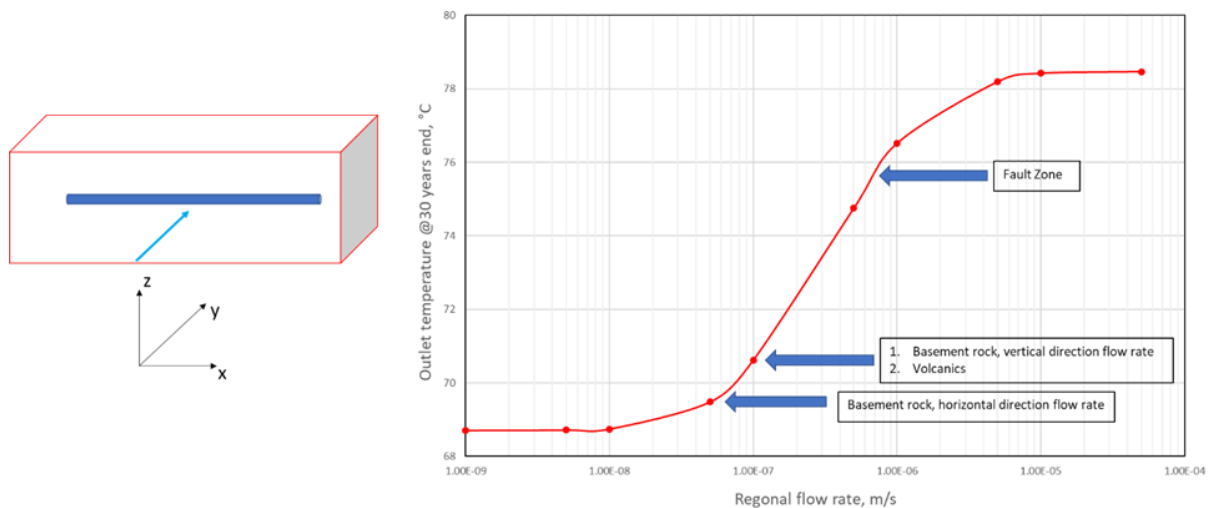


Figure 14 The outlet temperatures at the end of 30 years operation under different regional underground flow velocity.

7. CONCLUSIONS

In this study, we conducted thermodynamic modeling of the heat production performance of AGS using horizontal and inclined wellbore systems. The vertical injection and production wellbore are modeled by Duhamel's convolution method with the consideration of the heat exchange during the vertical wellbores. Modified natural coupling method is developed to model the multilateral inclined wellbore system by using coordinate rotation. Geothermal gradient is also considered in the modeling of the inclined well system to address the temperature vertical heterogeneity feature in this system. Key geometry parameters of this inclined well system are captured in the modeling for further sensitivity analysis. The results show the inclined wellbore can provide higher outlet working fluids temperature over 30 years, and this kind of advantage is decreasing over years. Due to the dense wellbore completion of the AGS with the inclined well system, the wellbore interference effect will significantly reduce the overall ability of the heat extraction. Especially in the late heat production phase, the heat production performance of the multilateral cases may be worse than the single lateral case and traditional horizontal well system. Larger dip angle and longer lateral wellbore length cannot solve the problem well. The wellbore interference of the multilateral completion comes from two reasons. The internal descending and ascending wells, and the nearby inclined well pairs both affect each other. At least 50 m spacing distance on the above two directions could help minimize the interference issue in the multilateral completion cases. Under suitable geological properties and ideal wellbore spacing distance, a 2000 m long inclined well system of 10-lateral AGS using 45° dip angle can provide 15 MWth heat energy at the first year and generate over 12 MWth heat energy over the rest 30 years operation. Compared with the same setting of horizontal well system, 3 MWth more heat energy can be generated by this inclined well system. Our results also show that the AGS may have enhanced heat production by induced convective heat flow. The underground water flow will also contribute to higher outlet temperature when deploying the AGS in hydrothermal system.

ACKNOWLEDGEMENT

This work originated as an independent evaluation of the Advanced Geothermal System by the inclined well system and is an output of the Geoscience for New Energy Supply (GNES) Program of Natural Resources Canada. Office of Energy Research and Development (OERD) provided funding for this study.

REFERENCES

- Beckers, K. F., Rangel-Jurado, N., Chandrasekar, H., Hawkins, A. J., Fulton, P. M., & Tester, J. W., 2022. Techno-Economic Performance of Closed-Loop Geothermal Systems for Heat Production and Electricity Generation. *Geothermics*, 100, 102318. <https://doi.org/10.1016/j.geothermics.2021.102318>.
- Canada Energy Regulator (CER), 2018. The Economics of Solar Power in Canada. <https://www.cer-rec.gc.ca/en/data-analysis/energy-commodities/electricity/report/solar-power-economics/index.html>.
- Eavor Technologies Inc., 2022. Available on the Internet: <https://eavor.com/about/technology>.
- EIA, 2014, Monthly generator capacity factor data now available by fuel and technology. Available on the Internet: <https://www.eia.gov/todayinenergy/detail.php?id=14611#>.
- Faes, W., Lecompte, S., van Bael, J., Salenbien, R., Bäbller, R., Bellemans, I., Cools, P., de Geyter, N., Morent, R., Verbeken, K., & de Paepe, M., 2019. Corrosion behaviour of different steel types in artificial geothermal fluids. *Geothermics*, 82, 182–189. <https://doi.org/10.1016/j.geothermics.2019.05.018>.

- Ghavidel, A., Gracie, R., & Dusseault, M. B., 2021. Transient heat transfer in a horizontal well in hot dry rock – Model, solution, and response surfaces for practical inputs. *Applied Thermal Engineering*, 195, 117158. <https://doi.org/10.1016/j.applthermaleng.2021.117158>.
- Government of Canada (GC), 2021. Net-Zero Emissions by 2050. Available on the Internet: <https://www.canada.ca/en/services/environment/weather/climatechange/climate-plan/net-zero-emissions-2050.html>.
- Government of Canada (GC), 2022. About Renewable Energy. Available on the Internet: <https://www.nrcan.gc.ca/our-natural-resources/energy-sources-distribution/renewable-energy/about-renewable-energy/7295>.
- Grasby, S.E., Allen, D.M., Bell, S., Chen, Z., Ferguson, G., Jessop, A., Kelman, M., Ko, M., Majorowicz, J., Moore, M., Raymond, J., and Therrien, R., 2011. Geothermal Energy Resource Potential of Canada, Geological Survey of Canada, Open File 6914, 322 p. doi:10.495/288745.
- International Energy Agency (IEA), 2021. Net Zero by 2050, IEA, Paris. Available on the Internet: <https://www.iea.org/reports/net-zero-by-2050>.
- Karlsdottir, S. N., 2021. Corrosion, Scaling and Material Selection in Geothermal Power Production. In Reference Module in Earth Systems and Environmental Sciences. Elsevier. <https://doi.org/10.1016/B978-0-12-819727-1.00106-0>.
- Kämmlein, M., & Stollhofen, H., 2019. Lithology-specific influence of particle size distribution and mineralogical composition on thermal conductivity measurements of rock fragments. *Geothermics*, 80, 119–128. <https://doi.org/10.1016/j.geothermics.2019.03.001>.
- Kilpatrick, R., 2017. Effect of Cold Climate on Wind Energy Production in Canada (2010 – 2016). NRCan Canada. Available on the Internet: <https://www.nrcan.gc.ca/maps-tools-publications/publications/energy-publications/publications/effect-cold-climate-wind-energy-production-canada-2010-2016/20369>.
- Morales-Simfors, N., & Bundschuh, J., 2022. Arsenic-rich geothermal fluids as environmentally hazardous materials – A global assessment. *Science of The Total Environment*, 817, 152669. <https://doi.org/10.1016/j.scitotenv.2021.152669>.
- Shao, H., Hein, P., Sachse, A., & Kolditz, O., 2016. *Geoenergy Modeling II*. Springer International Publishing. <https://doi.org/10.1007/978-3-319-45057-5>.
- Tester, J. W., Anderson, B. J., Batchelor, A. S., Blackwell, D. D., & DiPippo, R., 2006. The Future of Geothermal Energy - Impact of Enhanced Geothermal Systems (EGS) on the United States in the 21st Century. Massachusetts Institute of Technology. ISBN: 0-615-13438-6. Available from the Internet: www1.eere.energy.gov/geothermal/pdfs/future_geo_energy.pdf.
- Yuan, W., Chen, Z., Grasby, S. E., & Little, E., 2021. Closed-loop geothermal energy recovery from deep high enthalpy systems. *Renewable Energy*, 177. <https://doi.org/10.1016/j.renene.2021.06.028>.
- Zhang, Y., Yu, C., Li, G., Guo, X., Wang, G., Shi, Y., Peng, C., & Tan, Y., 2019. Performance analysis of a downhole coaxial heat exchanger geothermal system with various working fluids. *Applied Thermal Engineering*, 163(September), 114317. <https://doi.org/10.1016/j.applthermaleng.2019.114317>.